Cellular/Molecular

Non-NMDA-Type Glutamate Receptors Are Essential for Maturation But Not for Initial Assembly of Synapses at *Drosophila* Neuromuscular Junctions

Andreas Schmid,[1]* Gang Qin,[1]* Carolin Wichmann,[1,2] Robert J. Kittel,[1] Sara Mertel,[1] Wernher Fouquet,[1] Manuela Schmidt,[1] Manfred Heckmann,[2] and Stephan J. Sigrist[1,3]

[1]European Neuroscience Institute Göttingen, 37077 Göttingen, Germany, and [2]Institut für Klinische Neurobiologie, Universität Würzburg, and [3]Institut für Klinische Neurobiologie, Rudolf-Virchow Zentrum, Universität Würzburg, 97080 Würzburg, Germany

The assembly of glutamatergic postsynaptic densities (PSDs) seems to involve the gradual recruitment of molecular components from diffuse cellular pools. Whether the glutamate receptors themselves are needed to instruct the structural and molecular assembly of the PSD has hardly been addressed. Here, we engineered *Drosophila* neuromuscular junctions (NMJs) to express none or only drastically reduced amounts of their postsynaptic non-NMDA-type glutamate receptors. At such NMJs, principal synapse formation proceeded and presynaptic active zones showed normal composition and ultrastructure as well as proper glutamate release. At the postsynaptic site, initial steps of molecular and structural assembly took place as well. However, growth of the nascent PSDs to mature size was inhibited, and proteins normally excluded from PSD membranes remained at these apparently immature sites. Intriguingly, synaptic transmission as well as glutamate binding to glutamate receptors appeared dispensable for synapse maturation. Thus, our data suggest that incorporation of non-NMDA-type glutamate receptors and likely their protein–protein interactions with additional PSD components triggers a conversion from an initial to a mature stage of PSD assembly.

Key words: Drosophila; **NMJ; synaptogenesis; PSD; glutamate receptor; adhesion**

Introduction

Ionotropic glutamate receptors, subdivided into NMDA receptors and non-NMDA receptors, dominate excitatory synaptic transmission in our brain. Thereby, glutamatergic transmission is supported by a specialized postsynaptic subcellular organization, called the postsynaptic density (PSD). The PSD is involved in clustering and anchoring of postsynaptic receptors and ion channels and contains a specialized submembranous cytoskeleton with a rich collection of structural proteins that serve to organize this membrane specialization (Kim and Sheng, 2004). In contrast to the assembly of presynaptic active zones involving the delivery of prefabricated transport packets (Garner et al., 2002), postsynaptic assembly seems to depend on gradual *de novo* clustering of component proteins (Bresler et al., 2004). Synaptic non-NMDA receptors may either be recruited into PSDs from a diffuse plasma membrane pool by lateral migration (Borgdorff and Choquet, 2002) or be incorporated via subunit-specific constitutive or activity-dependent pathways (Bredt and Nicoll, 2003), potentially using preformed slots established at the postsynaptic membrane (Barry and Ziff, 2002). Rapid modulations of synaptic receptor number, considered the key for plasticity of glutamatergic synapses, might involve cytoplasmic receptor-bearing vesicles and exocytotic and endocytotic mechanisms (Malinow and Malenka, 2002), and allow the activation of previously "silent" synapses (Isaac, 2003).

Notably, recent reports also imply non-NMDA receptors in the formation and stability of larger postsynaptic subcellular compartments such as dendritic spines independent of their ionic transmission (Kasai et al., 2003; Passafaro et al., 2003). However, whether and if so where within the likely multistep PSD assembly process non-NMDA-type glutamate receptors are needed, remains unknown.

The neuromuscular junction of *Drosophila* (NMJ) allows for the efficient genetic analysis of development, plasticity, and function of glutamatergic synapses (Jan and Jan, 1976; Keshishian et al., 1996; Prokop, 1999; Koh et al., 2000; Richmond and Broadie, 2002). The glutamate receptor subunits expressed at the NMJ are related to mammalian non-NMDA-type glutamate receptors, and glutamate receptor levels can control the number of synapses forming at the NMJ (Petersen et al., 1997; Sigrist et al., 2000, 2002, 2003; Marrus et al., 2004). Thereby, the formation and growth of individual synapses is directly correlated with the entry of glutamate receptors from diffuse extrasynaptic pools, and in contrast to several other postsynaptic proteins tested, glutamate receptors stably integrate into immature PSDs (Rasse et al., 2005).

Received June 27, 2006; revised Aug. 22, 2006; accepted Sept. 19, 2006.

This work was supported by Center of Molecular Physiology of the Brain Deutsche Forschungsgemeinschaft Grants SFB 406, HE 2621/4-1, and SI 849/2-1 (A.S., R.J.K., M.H., S.J.S.). We thank C. O'Kane for TNT strains and A. Prokop for introduction to embryonic dissection.

*A.S. and G.Q. contributed equally to this work.

Correspondence should be addressed to Stephan J. Sigrist at the above address. E-mail: ssigris@gwdg.de.

G. Qin's present address: Max-Planck-Institut für Biochemie, Am Klopferspitz 18, 82152 Martinsried, Germany.

DOI:10.1523/JNEUROSCI.2722-06.2006

 0270-6474/06/2611267-11$15.00/0

Here, we start from the observation that *Drosophila* larvae still survived with extremely reduced levels of muscle glutamate receptors, hardly detectable by immunocytochemistry. We show by ultrastructural and molecular analysis that maturation of PSDs appeared defective in several aspects. We suggest that, during synapse formation, glutamate receptors incorporating into the postsynaptic membrane are critical to enlarge PSDs by organizing cell adhesion to bring presynaptic and postsynaptic membranes in apposition. Such a mechanism could be the basis for glutamate receptor levels to control the formation of synapses as well as subsynaptic compartments.

Materials and Methods

Molecular biology. A genomic construct of *gluRIIA* (Qin et al., 2005) was used for all clonings. The *gluRIIA* C-terminal deletion $gluRIIA^{\Delta C53}$ was produced by circular PCR leaving out the respective end of the C terminus without truncating the 3′-untranslated region (UTR) region (primers: 5′-TAGGTGGTCGGAATATTGGACG-3′ and 5′-AGTCACTCGCTCCTCCACCG-3′). The PCR product was blunt-end ligated and inserted into pUAST via *Eco*RI/*Xho*I. $gluRIIA^{Q614R}$ and $gluRIIA^{E783A}$ (both genomic constructs) were produced by two-step overlap extension PCRs (30 ± 2 overlapping bases) using Elongase (Stratagene, La Jolla, CA) and the following oligos: 5′-GCAGCGCATCCACTTCAACCT-3′ and 5′-TACCCAAATGCGCTATCTGTGTTCT-3′ for both $gluRIIA^{Q614R}$ and $gluRIIA^{E783A}$; 5′-CTAGGCAGAATGTCGCAGCCCTGTCTCATAATGGAGCCCACCATCAGCCAAG-3′ and 5′-CTTGGCTGATGGTGGGCTCCATTATGAGACAGGGCTGCGACATTCTGCCTAG-3′ for $gluRIIA^{Q614R}$ only; 5′-CGTGTCCATTCTCCAGCTGAGCGCCAGGGGCGAGCTGCAGAAGATG-3′ and 5′-CATCTTCTGCAGCTCGCCCCTGGCGCTCAGCTGGAGAATGGACACG-3′ for $gluRIIA^{E783A}$ only. PCR fragments were inserted into the *gluRIIA* backbone via *Bgl*II/*Nco*I and finally cloned into pUAST. All constructs were double-strand sequenced.

Genetics. The generation of animals expressing glutamate receptor IIA (GluRIIA), which lacks most of the 3′-untranslated region ($gluRIIA^{hypo}$), was described previously (Qin et al., 2005). *gluRIIA&IIB* double mutants ($gluRIIA^{null}IIB^{null}$) were described before (Petersen et al., 1997; DiAntonio et al., 1999; Qin et al., 2005). *gluRIIC* (*gluRIII*) mutants were established by crossing $gluRIII^{1}$ to $df(2L)ast^{4}$ (Marrus et al., 2004). Leaky expression of GluRIIC (IIC^{hypo}) was performed as described previously (Marrus and DiAntonio, 2004).

The genomic transgenes *gluRIIA*, $gluRIIA^{hypo}$, $gluRIIA^{\Delta C53}$, $gluRIIA^{Q614R}$, and $gluRIIA^{E783A}$, all established in df(2L)cl^{h4} background, were crossed to $df(2L)gluRIIA\&IIB^{SP22}$ to bring them into the $gluRIIA^{null}IIB^{null}$ background.

For activity suppression experiments, the following crosses were performed: *elav-gal4* with *UAS-tnt*, *ok319-gal4* with *UAS-tnt*, *cha-gal4* with $UAS\text{-}shi^{TS1}$ (raised at 29°C) and $df(2L)cl^{h4}$,$gluRIIA^{hypo}$;*elav-gal4* with df(2L)gluRIIA&B^{SP22},UAS-tnt. $shibire^{TS1}$ embryos were collected for 2 h, aged 12 h at 25°C, and then shifted to the restrictive temperature of 32°C until dissection.

CAC^{GFP} was expressed in $gluRIIA^{hypo}$ background by crossing $df(2L)gluRIIA\&B^{SP22}$,*ok6-gal4* to df(2L)cl^{h4},gluRIIA^{hypo};UAS-cac^{GFP}. *ok6-gal4* crossed to $UAS\text{-}cac^{GFP}$ served as control.

As wild type control w^{1} was used. Rescue embryos and larvae were selected using GFP-marked balancer chromosomes. If not indicated differently, all animals were raised at 25°C.

Immunohistochemistry. Primary antibodies were used at the following concentrations: mouse anti-GluRIIA (8B4D2; Developmental Studies Hybridoma Bank, University of Iowa, Iowa City, IA), 1:100; rabbit anti-GluRIIC, 1:500; mouse Nc82 (gift from E. Buchner, University of Würzburg, Würzburg, Germany), 1:100; rabbit anti-p21-activated kinase (PAK) (gift from N. Harden, Simon Fraser University, Burnaby, British Columbia, Canada), 1:2000; rabbit anti-α-Adaptin (gift from M. Gonzalez-Gaitan, MPI of CBG, Dresden, Germany), 1:50; mouse anti-fasciclin II (FasII) (1D4; Developmental Studies Hybridoma Bank), 1:50; mouse anti-Dlg (Developmental Studies Hybridoma Bank), 1:500; and goat anti-HRP cyanine 5, 1:200.

Styryl dye labeling. FM5-95 labeling was done as described previously (Rasse et al., 2005).

Electrophysiology. Two-electrode voltage-clamp recordings were performed at 22°C from muscle fiber 6 of abdominal segments 2 and 3 of late third-instar larvae as described previously (Qin et al., 2005). The composition of the extracellular hemolymph-like saline (HL-3) (Stewart et al., 1994) was as follows (in mM): 70 NaCl, 5 KCl, 20 $MgCl_2$, 10 $NaHCO_3$, 5 trehalose, 115 sucrose, 5 HEPES, 1 $CaCl_2$, pH adjusted to 7.2. For paired-pulse recordings, the interpulse interval was 19.5 ms and 4 s rest was left between sweeps. The rise time and decay time constant (τ) were obtained from the average event at 0.2 Hz stimulation. The rise time was measured from 10 to 90% of the maximum amplitude, and the decay was fit with a single exponential function from 60% of the peak. All recordings consisted of 20 traces per cell. Stimulation artifacts of evoked excitatory junctional currents (eEJCs) were removed for clarity.

Transmission electron microscopy. Dissected preparations of third-instar larvae (NMJ 6/7; segment A2/A3) were primary fixed in a mixture of 4% paraformaldehyde and 0.5% glutaraldehyde in 0.1 M PBS, pH 7.2, for 10 min and additionally fixed 60 min on ice with secondary fixative comprising 2% glutaraldehyde in 0.1 M sodium cacodylate buffer, pH 7.2, washed three times for 5 min in sodium cacodylate buffer and postfixed on ice for 1 h with 1% osmium tetroxide (in 0.1 M sodium cacodylate buffer), followed by a 1 h washing step in sodium cacodylate buffer and three brief washing steps in distilled water. The samples were stained en bloc with 1% uranyl acetate in distilled water for 1 h on ice. After a brief wash with distilled water, samples were dehydrated at room temperature in increasing ethanol concentrations, infiltrated in Epon resin (100% EtOH/Epon 1:1, 30 and 90 min; 100% Epon, overnight), and embedded for 24 h at 85°C. The samples were trimmed, and series of 80–90 nm ultrathin sections were cut with a 35° diamond knife (Diatome, Biel, Switzerland) on a Reichert Ultracut Ultramicrotome (Leica, Nussloch, Germany) and mounted on Formvar-coated grids. The sections were stained in uranyl acetate and lead citrate. Pictures were taken with a Philips (Mahwah, NJ) EM 301 transmission electron microscope.

Dissection and immunostainings. Embryonic (stage 17; 20–22 h old) and larval dissections were performed as recently described (Qin et al., 2005). The dissected samples were fixed either for 10 min with 4% paraformaldehyde in PBS or for 5 min with ice-cold methanol (for 8B4D2 stainings), and then incubated with primary antibodies overnight. The next day, fluorescence-labeled secondary antibodies (Dianova, Hamburg, Germany) were applied for 2 h, and the dissections were mounted in VectaShield mounting medium (Vector Laboratories, Burlingame, CA).

Imaging. In vivo imaging experiments were done as described recently (Rasse et al., 2005). Imaging of embryonic and larval body-wall preparations was either performed on a Zeiss (Oberkochen, Germany) Axioscope with Axiocam camera, using a 100× oil objective of numerical aperture 1.4. or on a Leica DM IRE2 microscope equipped with a Leica TCS SP2 AOBS scan head, using a Leica HCX PL Apo CS, 63×, 1.32 numerical aperture oil objective.

Image analysis and statistics. To determine the PSD size (see Fig. 3*J*,*K*), maximum projections of confocal *z*-stacks were subjected to background correction, Gaussian blur filtering, and normalization of the maximum pixel intensity. To determine the size of single PSDs (here visualized by PAK immunostainings of NMJ 4), manual PSD segmentation was used. Subsequently, the image was filtered (A trous filter) and a threshold of 50 (gray value) was applied. The resulting binary image was inverted to obtain a binary mask, which was superimposed (minimum overlay) with the original maximum projection. Finally, the remaining particles were counted and analyzed for their pixel number, which was converted to square micrometers. To quantify the distribution of FasII relative to PAK, the intensity profile along the maximum diameter of the respective PSD was plotted (profile length, 1 μm). In both cases, 20 intensity profiles were averaged. Analysis of synaptic membranes visualized by electron micrographs was performed manually by classifying the presynaptic and postsynaptic membrane according to their electron dense character and their linear apposition. Subsynaptic reticulum (SSR) thickness was determined as described previously (Gorczyca et al., 1999) from electron micrographs of midbouton sections. All image analysis was performed

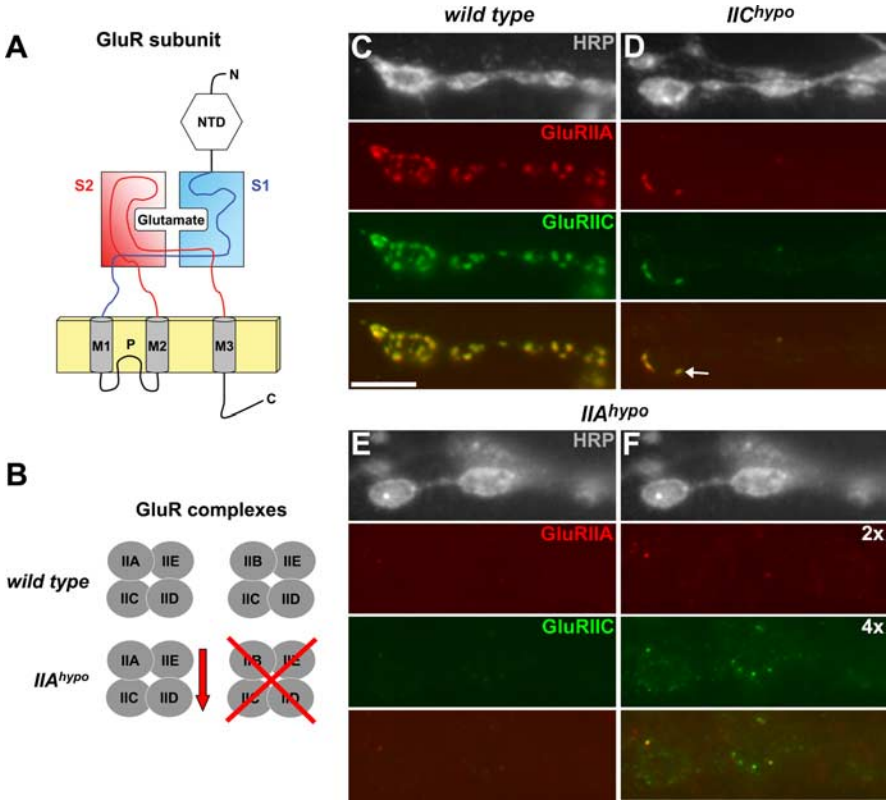

Figure 1. Larval NMJs with extremely reduced levels of postsynaptic glutamate receptors. ***A***, Schematic view of a glutamate receptor subunit. Abbreviations: NTD, N-terminal domain; S1 and S2, glutamate binding domains; M1–3, transmembrane domains; P, reentrant pore loop. ***B***, Two different glutamate receptor complexes are thought to form at the NMJ, incorporating GluRIIC, GluRIID, and GluRIIE together with either GluRIIA or GluRIIB. In *gluRIIA*^{hypo} (*IIA*^{hypo}) animals, the embryonic lethal *gluRIIA*^{null}*IIB*^{null} situation was rescued by a *gluRIIA* genomic transgene lacking 3′-UTR sequences, resulting in a severe deprivation of GluRIIA and a complete lack of GluRIIB complexes. ***C–F***, Shown are epifluorescence images of NMJs of muscles 6/7 from *gluRIIA*^{hypo} (***E***, ***F***), *gluRIIC*^{hypo} (*IIC*^{hypo}) (see Results, Formation of glutamatergic NMJ synapses deprived of postsynaptic glutamate receptors) (***D***), and wild-type third-instar larvae (***C***). Stainings are against GluRIIA (red) and GluRIIC (green). ***C–E*** have identical exposure times, and in ***F***, exposure times were two or four times longer. All images were taken with wide-field microscopy. Scale bar, 5 μm.

using NIH ImageJ. Adobe Photoshop (Adobe Systems, San Jose, CA) was used for figure compilation.

The nonparametric Mann–Whitney rank sum test was generally used for statistical analysis. The data are reported as mean ± SEM, *n* indicates the sample number, and *p* denotes the significance: $^{*}p < 0.05$, $^{**}p < 0.01$, $^{***}p < 0.001$.

Results

Formation of glutamatergic NMJ synapses deprived of postsynaptic glutamate receptors

Previous work has identified a total of five glutamate receptor subunits (Fig. 1*A*, scheme) within *Drosophila* muscles (GluRIIA, IIB, IIC, IID, and IIE), from which two receptor complexes incorporating GluRIIC, GluRIID, and GluRIIE together with either GluRIIA or GluRIIB seem to form (Fig. 1*B*). GluRIIA or GluRIIB containing complexes coexist within individual synapses of the NMJ. In both *gluRIIA* or *gluRIIB* single mutants, structurally normal synapses form, meaning that either complex is per se dispensable for the formation of proper NMJ synapses (Petersen et al., 1997; DiAntonio et al., 1999; Marrus et al., 2004; Chen et al., 2005; Qin et al., 2005). In *gluRIIA&IIB* double mutants (*gluRIIA*^{null}*IIB*^{null}), however, and similarly in *gluRIIC*^{null}, *gluRIID*^{null}, and *gluRIIE*^{null} single mutants, all glutamate receptor subunits are absent from the NMJ, resulting in embryonic lethality (Petersen et al., 1997; Featherstone and Broadie, 2002; Marrus et al., 2004; Qin et al., 2005). However, already minimal amounts of the relevant glutamate receptors can rescue the lethality and even give rise to adult flies (Marrus and DiAntonio, 2004; Qin et al., 2005).

We started by studying the effects of glutamate receptor deprivation at the well described larval NMJ. Here, individual synapses are considerably larger than in the embryo (Rheuben et al., 1999), and moreover, our recent *in vivo* imaging study indicated a rate-limiting role for glutamate receptor incorporation in the formation of synapses at larval NMJs (Rasse et al., 2005). Three different situations combining a severe depression of glutamate receptor subunits still compatible with larval vitality have been described previously. When *gal4*-inducible cDNA constructs of either *gluRIIC* (Marrus and DiAntonio, 2004) or *gluRIID* (Qin et al., 2005) were brought into the corresponding single mutant background, "leaky expression" permitted larval survival in the absence of *gal4*-drivers. A strong reduction in the synaptic expression of all glutamate receptor subunits was observed for the *gluRIIC*^{hypo} (Fig. 1*D*) (Marrus and DiAntonio, 2004) and *gluRIID*^{hypo} (Qin et al., 2005) situation. In the third constellation, the otherwise lethal *gluRIIA*^{null}*IIB*^{null} situation could be rescued with a *gluRIIA* genomic transgene encoding the whole open reading frame but lacking parts of the 3′-UTR (from here on referred to as *gluRIIA*^{hypo}), resulting in <5% of wild-type GluRIIA mRNA levels and certainly no GluRIIB (Qin et al., 2005). Some PSDs obviously still showed normal size and glutamate receptor intensity at *gluRIIC*^{hypo} NMJs (Fig. 1*D*, arrow) (Marrus and DiAntonio, 2004). However, at larval NMJs of *gluRIIA*^{hypo}, no such PSDs could be observed (Fig. 1*E*). In fact, only when using atypically long exposure times very faint residual accumulations of GluRIIA and GluRIIC could be visualized (Fig. 1*F*). Thus, because of their extreme and consistent reduction of glutamate receptors, we concentrated on *gluRIIA*^{hypo} larvae to study the formation of glutamatergic synapses mostly deprived of glutamate receptors.

Presynaptic release sites are functionally and structurally maintained at glutamate receptor-deprived NMJ synapses

We went on to further investigate NMJ synapses developing in the near absence of glutamate receptors by using molecular markers. The active zone (AZ) is a specialized presynaptic region, where synaptic vesicles dock, fuse, and release their neurotransmitters (Zhai and Bellen, 2004). In *Drosophila*, AZs are associated with electron dense specializations (T-bars) (Atwood et al., 1993; Zhai and Bellen, 2004). The monoclonal antibody Nc82 was shown to label the AZs of *Drosophila* synapses (Wucherpfennig et al., 2003) by recognizing the Bruchpilot protein (BRP), which is essential for T-bar formation (Atwood, 2006; Kittel et al., 2006; Wagh et al., 2006). At *gluRIIA*^{hypo} synapses, the density and size of synaptic clusters of both Nc82 (supplemental Fig. S1*B*, available

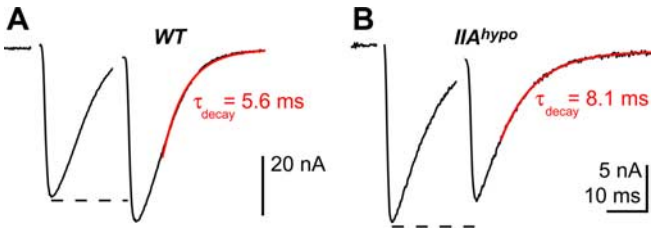

Figure 2. Indications of chronically increased release probability at glutamate receptor-deprived NMJ synapses. Shown are average eEJC traces of wild-type (***A***) and *gluRIIA*^{hypo} (***B***) larval NMJs after paired-pulse stimulation (interpulse interval, 19.5 ms). eEJCs of *gluRIIA*^{hypo} were strongly reduced in amplitude as described previously (Qin et al., 2005) and showed an untypical paired-pulse depression and an increased decay τ (wild type, 1.18 ± 0.04, $n = 7$; *gluRIIA*^{hypo}, 0.83 ± 0.05, $n = 11$, $p = 0.003$; decay τ: wild type, 4.96 ± 0.42 ms, $n = 12$; *gluRIIA*^{hypo}, 6.73 ± 0.62 ms, $n = 11$, $p = 0.013$).

at www.jneurosci.org as supplemental material) and Ca^{2+} channels (supplemental Fig. S1*D*, available at www.jneurosci.org as supplemental material) appeared unaffected when compared with wild-type controls (supplemental Fig. S1*A*,*C*, available at www.jneurosci.org as supplemental material). Thus, consistent with the presence of T-bars (see below in Fig. 4), AZ structures seemed to establish normally at *gluRIIA*^{hypo} synapses. AZs are also surrounded by zones of endocytosis, which can be labeled in α-Adaptin stainings (Dornan et al., 1997). The distribution of α-Adaptin appeared unchanged as well (supplemental Fig. S1*B*, available at www.jneurosci.org as supplemental material). Thus, in contrast to the PSD (see below in Figs. 3, 4), the molecular and structural composition of the presynaptic AZs seemed unaffected.

Are these AZs still functional? We first found that *gluRIIA*^{hypo} larvae were only moderately limited in mobility. Moreover, styryl dye (FM5-95) incorporation after high-frequency stimulation (Kuromi and Kidokoro, 2002; Wucherpfennig et al., 2003) showed that vesicle release persisted at *gluRIIA*^{hypo} NMJs (supplemental Fig. S1*F*, available at www.jneurosci.org as supplemental material). In a previous electrophysiological analysis we had shown that nerve evoked excitatory junctional currents at *gluRIIA*^{hypo} NMJs are reduced to ~30% of the wild-type level. Notably, in this genotype, miniature excitatory junctional currents, indicating the postsynaptic glutamate sensitivity at individual synapses, were below the detection threshold, which we estimate to be at ~20% of the wild-type amplitude (Qin et al., 2005). Thus, after an action potential, the number of presynaptically released vesicles is likely increased as part of a presynaptic compensation for reduced postsynaptic sensitivity (Petersen et al., 1997; Reiff et al., 2002). In fact, paired-pulse stimulation at these junctions led to an atypical depression as would be expected for a synaptic system with a chronic increase in presynaptic release probability (Fig. 2*A*,*B*) (wild-type control: 1.18 ± 0.04, $n = 7$; *gluRIIA*^{hypo}: 0.83 ± 0.05, $n = 11$; $p = 0.003$). In addition, we recognized that the decay time constant (τ) of evoked responses was increased (Fig. 2*A*,*B*) (wild-type control: 4.96 ± 0.42 ms, $n = 12$; *gluRIIA*^{hypo}: 6.73 ± 0.62 ms, $n = 11$; $p = 0.013$), potentially pointing toward changes in glutamate clearance or atypical functional properties of the glutamate receptors remaining at these synapses. The rise time of evoked junctional currents was not significantly altered (wild-type control: 1.08 ± 0.05 ms, $n = 12$; *gluRIIA*^{hypo}: 1,17 ± 0.08 ms, $n = 11$; $p = 0.498$). In summary, AZs still formed at the presynaptic site of NMJ synapses deprived of glutamate receptors. These AZs appeared fully active in vesicle release, and likely vesicle release is even increased to compensate for the drastically reduced postsynaptic glutamate sensitivity. Such a compensation was described before for *gluRIIA* mutants, which notably show a less drastic drop in postsynaptic glutamate sensitivity (Petersen et al., 1997).

Early stop of postsynaptic maturation at glutamate receptor-deprived NMJ synapses

Next, we were interested in analyzing postsynaptic assembly at glutamate receptor-deprived synapses. The PAK kinase forms a complex with PAK-interactive exchange factor (PIX) and Rac, involved in aspects of PSD assembly (Albin and Davis, 2004). PAK widely serves as a PSD marker at NMJ synapses and strictly colocalizes with the glutamate receptor subunit GluRIIA (Rasse et al., 2005). The size of PAK signals at individual PSDs seemed strongly reduced in *gluRIIA*^{hypo} animals (Fig. 3, compare *C*, *D*). In fact, quantification of *gluRIIA*^{hypo} NMJs of mature third-instar larvae showed a significant reduction in the size of PAK signals (Fig. 3*J*) (wild type, 0.385 ± 0.005 μm^2, $n = 1709$, six NMJs; *gluRIIA*^{hypo}, 0.311 ± 0.006 μm^2, $n = 1014$, seven NMJs; $p < 0.0001$), whereas the density of PSDs (identified as PAK spots) over the NMJ surface appeared unchanged.

In principle, the observed molecular defects in postsynaptic assembly might not reflect a genuine inability to form mature PSDs but instead a deficit in maintenance of matured PSDs (and thus "defective synapses" would have accumulated until late larval development as predominantly analyzed in this study). However, also earlier during development, in first- (data not shown) and second-instar *gluRIIA*^{hypo} larvae, synaptic PAK signals were identically reduced (Fig. 3*H*,*K*) (quantification for second-instar: wild type, 0.358 ± 0.007 μm^2, $n = 699$, six NMJs; *gluRIIA*^{hypo}, 0.280 ± 0.006 μm^2, $n = 622$, six NMJs; $p < 0.0001$).

Reduced synaptic PAK signals pointed toward defects in the molecular and/or structural assembly of the PSD region of synapses lacking glutamate receptors. FasII, an NCAM (neural cell adhesion molecule)-related cell adhesion molecule, and Discs large (Dlg), founding member of the PSD-95-type MAGUK (membrane-associated guanylate kinase) family, take part in growth and maturation of the NMJ structure and interact molecularly (Schuster et al., 1996; Thomas et al., 1997; Zito et al., 1997). At wild-type NMJs, FasII and Dlg are highly enriched at the "perisynaptic" muscle membrane but are clearly reduced at the actual postsynaptic membrane (Fig. 3*A*,*C*,*G*). In *gluRIIA*^{hypo} larvae, however, FasII and Dlg did not appear reduced at postsynaptic membranes (Fig. 3*B*,*D*,*H*). In fact, quantification of FasII (Fig. 3*I*) demonstrated a distinct reduction of FasII staining intensity at postsynaptic sites (identified by PAK labeling, also note the decreased PAK spot size in *gluRIIA*^{hypo}) for wild type but a flat distribution at *gluRIIA*^{hypo} synapses (for numbers and details, see legend).

Hence, perisynaptic proteins such as the membrane protein FasII and the membrane-associated Dlg are now present in a membrane compartment normally destined to become postsynaptic membrane. We conclude that a lack of glutamate receptors interferes with the maturation of postsynaptic sites, and the molecular composition of these postsynaptic assemblies seemed to remain in an immature, nascent state.

Ultrastructural analysis: lack of apposition between presynaptic and postsynaptic membranes at NMJ synapses deprived of glutamate receptors

Defects in NMJ morphology became obvious in immunolabelings of *gluRIIA*^{hypo} NMJs (Fig. 4*C*). Both the number of boutons as well as the number of synapses per NMJ were reduced at

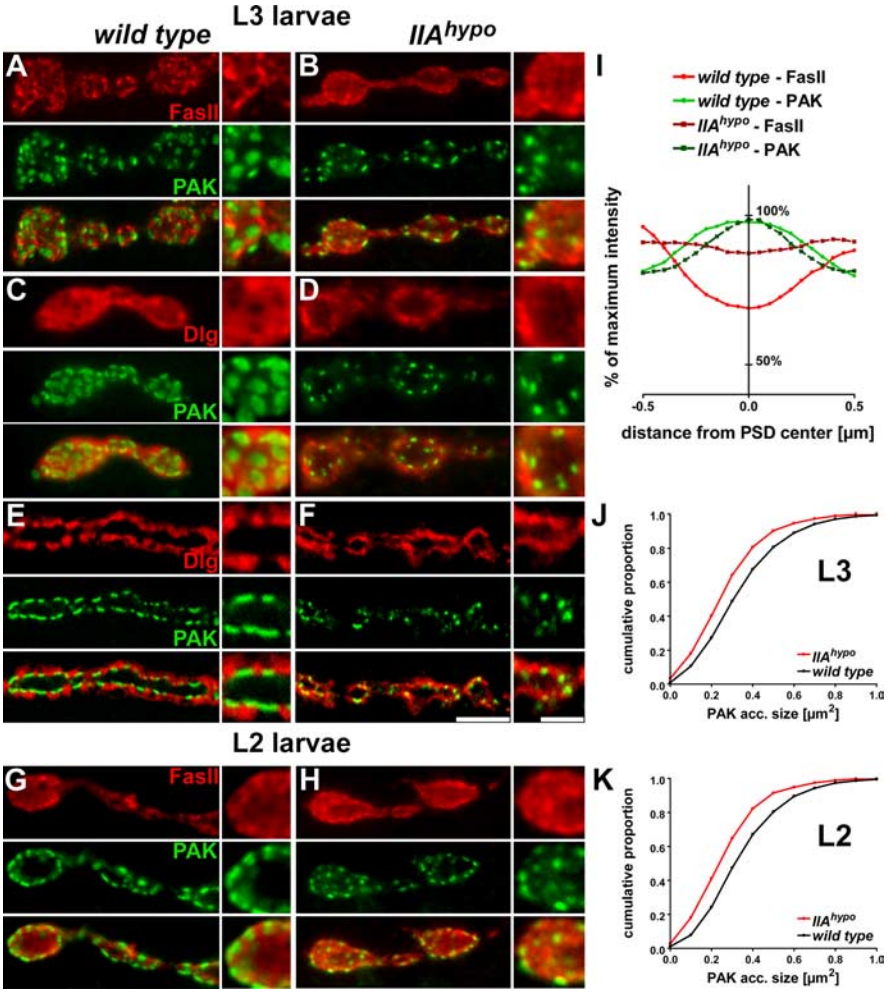

Figure 3. Molecular markers of postsynaptic assembly at glutamate receptor deprived NMJ synapses. ***A***, ***B***, At wild-type third-instar larval (L3) NMJs (***A***), FasII (red) is highly enriched in the perisynaptic membrane but reduced at synaptic membranes. FasII "holes" match the PSDs identified via PAK labeling (green). ***B***, Boutons of *gluRIIA*^{hypo}: atypically homogenous FasII distribution with either no or only very small holes at PAK sites. ***C***, ***D***, Dlg (red) shows perisynaptic distribution at wild-type boutons as well (***C***), but homogenous staining at *gluRIIA*^{hypo} boutons (***D***). ***E***, ***F***, Single confocal *z*-sections labeled for Dlg (red) and PAK (green), from wild-type (***E***) and *gluRIIA*^{hypo} NMJs (***F***). Note that thickness of postsynaptic Dlg signal was reduced in *gluRIIA*^{hypo} consistent with a decrease in SSR diameter as observed with electron microscopy (see below). ***G***, ***H***, Second-instar larval (L2) NMJs of *gluRIIA*^{hypo} (***H***) and wild type (***G***). FasII (red) and PAK (green) showed a similar distribution as observed in third instar (***A***, ***B***). ***I***, Quantification of the FasII (red) and PAK (green) intensity profiles at single PSDs (0 μm: PSD center) of *gluRIIA*^{hypo} (dashed lines) and wild-type (solid lines) second-instar larvae. In *gluRIIA*^{hypo}, FasII showed a flat intensity profile, whereas in wild-type FasII, intensity was clearly reduced at the postsynaptic membrane marked by PAK (in PSD center: wild type, 74.7 $\pm$ 1.8%, $n = 20$; *gluRIIA*^{hypo}, 95.8 $\pm$ 1.5%, $n = 20$; $p < 0.0001$; percentages are relative to average intensity in neighboring perisynaptic segments). ***J***, ***K***, Size of synaptic PAK accumulations at *gluRIIA*^{hypo} (red) and wild-type (black) NMJs (muscle 4, 1b innervation) in larval stages L2 (***K***) and L3 (***J***). Scale bars: large panels, 5 μm; small panels, 2 μm.

gluRIIA^{hypo} NMJs (third instar, NMJ 4, Ib innervation; bouton number: wild type, 26.7 $\pm$ 2.5, $n = 6$, *gluRIIA*^{hypo}, 13.3 $\pm$ 1.9, $n = 7$, $p = 0.0047$; synapse number: wild type, 285 $\pm$ 16, $n = 6$, *gluRIIA*^{hypo}, 153 $\pm$ 17, $n = 7$, $p = 0.0023$). In addition, boutons often appeared abnormally round (Fig. 4*C*) and no longer polygonal as typically observed in wild type (Fig. 4*A*).

To further analyze how far postsynaptic differentiation was affected by the lack of glutamate receptors, NMJs of mature *gluRIIA*^{hypo} larvae were subjected to transmission electron microscopy (EM). Within NMJ terminals, synaptic vesicles and typical organelles such as mitochondria seemed unaffected. Moreover, presynaptic T-bars were found at apparently normal frequency (per midbouton section: wild type, 0.88 $\pm$ 0.13, $n = 8$; *gluRIIA*^{hypo}, 0.89 $\pm$ 0.26, $n = 9$; $p = 0.96$), consistent with the preservation of AZ function (see above). T-bars also enabled an unambiguous localization of synaptic sites within electron micrographs. Notably, the glutamate receptor-deprived synapses showed severe defects in membrane organization. Normally, presynaptic and postsynaptic membranes are more electron dense than neighboring extrasynaptic membranes, and show a flat and linear apposition, easily visualized in EM cross sections (Fig. 4*E*, arrows). This membrane apposition at mature synapses typically covers a few hundred nanometers, far exceeding the diameter of the attached T-bar (Fig. 4*E*). At *gluRIIA*^{hypo} NMJ synapses, however, presynaptic and postsynaptic membranes showed either no or only reduced electron density (Fig. 4*D*,*F–J*). Most notably, the area of close apposition between presynaptic and postsynaptic membrane was clearly reduced or sometimes totally absent at *gluRIIA*^{hypo} NMJ synapses (Fig. 4*F*, arrows;*G–J*). Instead, the membranes normally destined to show synapse-specific organization were of typical perisynaptic organization, which is characterized by the SSR that forms by pronounced infoldings of the muscle membrane only focally contacting the presynaptic neuronal plasma membrane (Gorczyca et al., 1999). Consistent with the decreased diameter of the Dlg-positive area surrounding boutons (Fig. 3*H*), the SSR was reduced in *gluRIIA*^{hypo} larvae (Fig. 4, compare *B*, *D*, white arrows) (Fig. 4*K*, SSR thickness, type Ib boutons: wild type, 684 $\pm$ 55 nm, $n = 7$; *gluRIIA*^{hypo}, 311 $\pm$ 13nm, $n = 9$; $p = 0.0047$).

Together, we conclude that glutamate receptors are directly or indirectly needed to confer proper molecular composition to synaptic membranes. In result, the mature apposition between presynaptic and postsynaptic membranes normally extending over a few hundred nanometers, and likely acting as a prerequisite for properly timed neurotransmission, could no longer be observed.

Initial molecular assembly of PSDs independent of glutamate receptors

We showed, that despite dramatic glutamate receptor deprivation, a residual postsynaptic assembly of NMJ synapses demonstrated by PAK localization still took place in *gluRIIA*^{hypo} larvae. At NMJs of *gluRIIA*^{hypo} embryos, glutamate receptors were not detectable (Fig. 5*C*), and indistinguishable from *gluRIIA*^{null}*IIB*^{null} NMJs in stainings (Fig. 5*B*). Nevertheless, as shown above, traces of residual glutamate receptor levels could be observed at larval NMJs of *gluRIIA*^{hypo} animals (Fig. 1*E*,*F*). In principle, these minimal glutamate receptor levels could be sufficient to establish the observed residual postsynaptic assembly, which in turn could suggest a role of glutamate receptors in initial PSD formation. To

address this question, PAK localization was studied at embryonic synapses fully lacking glutamate receptors [stage 17; 20–22 h after egg laying (AEL)]. However, at both *gluRIIC*^{null} (Fig. 5*E*) as well as *gluRIIA*^{null}*IIB*^{null} (Fig. 5*F*) NMJs, PAK still accumulated opposite presynaptic active zones, identified via Nc82 labeling, similar to wild-type synapses (Fig. 5*D*). Similarly, PAK also accumulated at NMJs of *gluRIIA*^{hypo} embryos (Fig. 5*G*). Thus, initial molecular assembly at prospective PSDs regions still seemed possible in the absence of postsynaptic glutamate receptor complexes.

Neurotransmission and glutamate-triggered ionic conductance are dispensable for NMJ synapse maturation and growth

So far, we showed that glutamate receptors are specifically needed to allow the maturation of the synaptic membrane organization. The question arose, whether the defects at synapses lacking glutamate receptors are mediated by the loss of synaptic transmission, resulting from the absence of glutamate receptors. To check whether a lack of synaptic transmission could in fact be responsible, several independent experimental strategies to block synaptic transmission were chosen. In larvae, tetanus toxin light chain (TNT) was expressed using the mosaic motoneuron driver line *ok319-gal4* (Sweeney et al., 1995). Such larvae appeared paralyzed, whereas in comparison locomotion defects in *gluRIIA*^{hypo} larvae were only moderate. However, NMJ synapses of these tetanus toxin expressing larvae had fully developed postsynaptic receptor fields (Fig. 6*C*). In addition, transgenic expression of temperature-sensitive, dominant-negative Dynamin (UAS-*shibire*^{TS1}) at 29°C with the *cha-gal4* driver was used to silence the cholinergic neurons "upstream" of motoneurons (Salvaterra and Kitamoto, 2001). This led to a severe paralysis of larvae, while again mature PSDs formed (Fig. 6*D*). Together, a severe blockade of NMJ transmission did not interfere with postsynaptic assembly.

It could be argued that, when tetanus toxin expression was driven by *ok319-gal4*, suppression of presynaptic release was not complete, as indicated by larval survival. Thus, we cannot exclude that in particular residual miniature events might be present (Sweeney et al., 1995). In principle, small residual levels of spontaneous activity, as likely present in the tetanus toxin-expressing larvae, might already be sufficient to allow postsynaptic assembly. In fact, miniature activity has been implicated in the formation of postsynaptic receptor fields in the embryo (Saitoe et al., 2002). However, this finding was discussed controversially (Featherstone and Broadie, 2002; Verstreken and Bellen, 2002). Complete suppression of synaptic release at the NMJ leads to late embryonic lethality in *Drosophila*. Thus, we studied the consequence of completely suppressing all synaptic transmission including miniature responses at the embryonic

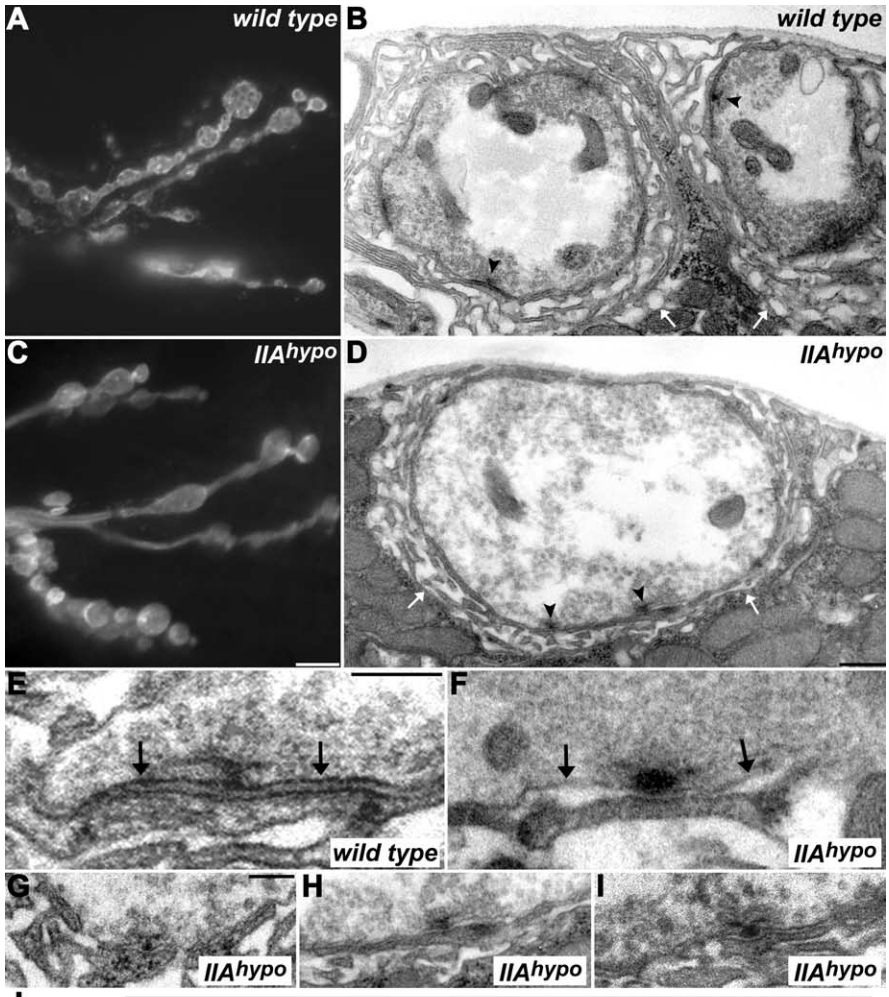

J

IIA^{hypo}	non-reduced	reduced	highly reduced
Electron density of synaptic membranes (n = 33)	0%	55%	45%
	full contact	defective	highly defective
Membrane apposition (n = 31)	4%	48%	48%

K

	wild type	IIA^{hypo}	
SSR thickness	684 ± 55 nm (n = 7)	311 ± 13 nm (n = 9)	p = 0.0002

Figure 4. Electron microscopic analysis of glutamate receptor-deprived NMJ synapses. ***A***, ***C***, HRP labelings of wild-type (***A***) and *gluRIIA*^{hypo} NMJs (***C***). Boutons of *gluRIIA*^{hypo} tend to be round and are often placed in large intervals along motoneuron branches. ***B***, ***D***, Transmission electron micrographs of wild-type (***B***) and *gluRIIA*^{hypo} (***D***) NMJs. Presynaptic T-bars were observed at apparently unchanged density (***B***, ***D***, arrowheads), whereas the typical electron dense character of synaptic membranes (***B***) was reduced at *gluRIIA*^{hypo} NMJs (***D***). SSR appeared reduced (***B***, ***D***, white arrows). ***E***, ***F***, High magnitude electron micrographs of wild-type (***E***) and *gluRIIA*^{hypo} (***F***) synapses. In wild type, presynaptic and postsynaptic membranes are characterized by a close apposition (***E***, arrows) and electron dense character. At *gluRIIA*^{hypo} synapses, membranes lacked electron density and membrane apposition (***F***, arrows). ***G–J***, Additional examples illustrating ultrastructural defects at *gluRIIA*^{hypo} synapses. ***J***, Estimation of ultrastructural defects at *gluRIIA*^{hypo} synapses. All analyzed *gluRIIA*^{hypo} synapses showed either moderate or complete loss of electron density, with only 1 of 31 *gluRIIA*^{hypo} synapses showing linear membrane apposition covering several hundred nanometers as typically observed in wild type ("full contact"). The remaining synapses showed strong or very strong defects in apposition between presynaptic and postsynaptic membranes. ***K***, Quantification of SSR thickness from EM cross sections. All shown images derived from type Ib innervations on muscles 6/7 or 12/13 of third-instar larvae. Scale bars: ***C***, 5 μm; ***D***, 500 nm; ***E***, ***G***, 200 nm.

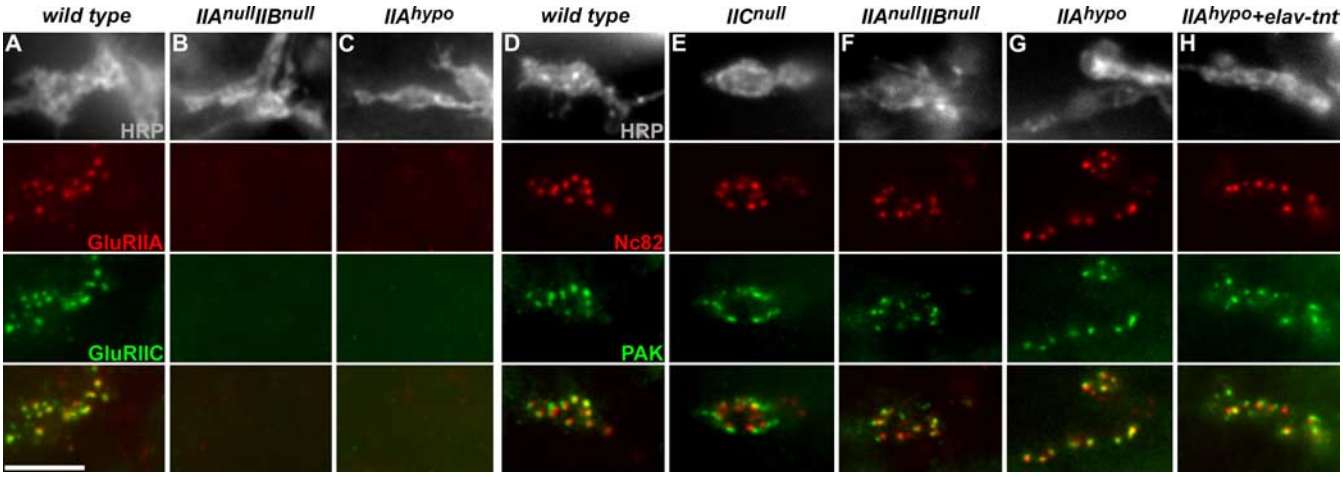

Figure 5. Synapse assembly at embryonic NMJs lacking glutamate receptors. ***A–C***, Embryonic *Drosophila* NMJs (stage 17) stained for HRP (gray), GluRIIA (red), and GluRIIC (green). Wild-type (***A***) NMJs showed synaptic expression of GluRIIA and GluRIIC, whereas, as expected, glutamate receptors were absent from NMJs of $gluRIIA^{null}IIB^{null}$ embryos (***B***). In $gluRIIA^{hypo}$ embryos (***C***), glutamate receptors were below detection limit as well. ***D–H***, Despite the absence of glutamate receptors, embryonic NMJs of $gluRIIC^{null}$ (***E***) and $gluRIIA^{null}IIB^{null}$ (***F***) animals still showed accumulations of the PSD marker PAK (green) opposite presynaptic release sites labeled with Nc82 (red) similar to wild type (***D***). PAK also accumulated at $gluRIIA^{hypo}$ NMJ synapses with (***H***) or without (***G***) a concomitant block of presynaptic activity through pan-neuronal expression of tetanus-toxin (*elav-tnt*). Scale bar, 5 μm.

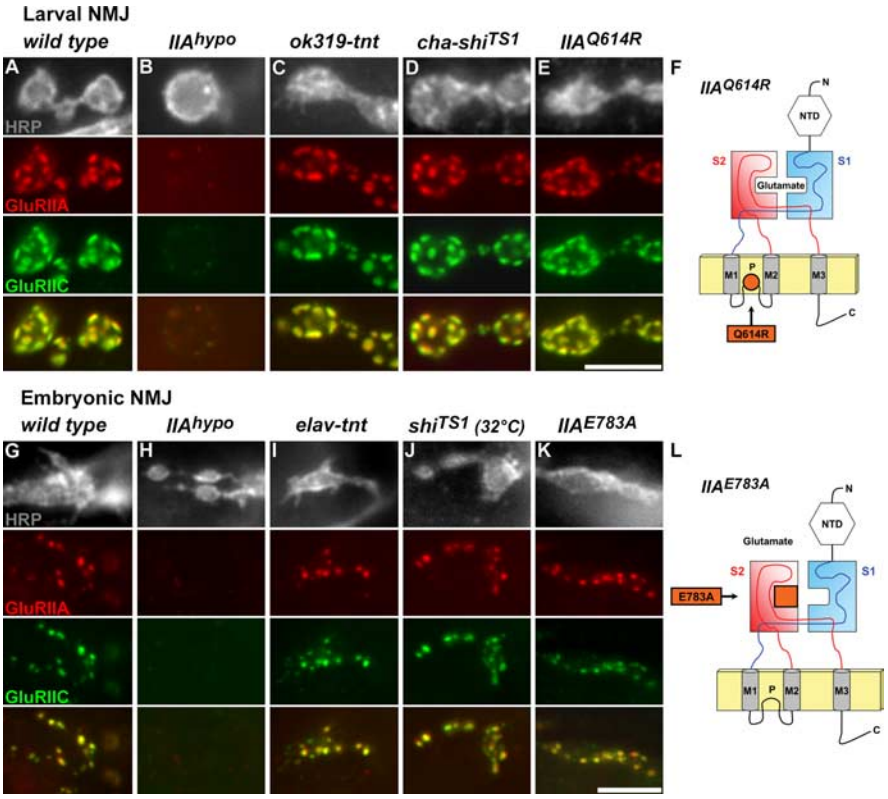

Figure 6. NMJ synapse assembly after suppression of neurotransmission or glutamate receptor ligand binding. ***A–E***, Stainings of third-instar NMJs (muscle 6/7) for HRP (gray), GluRIIA (red), and GluRIIC (green). Shown are controls (***A***), $gluRIIA^{hypo}$ (***B***), larvae expressing either tetanus toxin with the mosaic motoneuron driver *ok319-gal4* (***C***) or $shibire^{TS1}$ in cholinergic neurons (***D***) (at 29°C), and a pore-modified version of GluRIIA ($gluRIIA^{Q614R}$) (***E***) expressed in the $gluRIIA^{null}IIB^{null}$ background. ***F***, Scheme of GluRIIA ^{Q614R}: a genomic *gluRIIA* clone with the exchange Q614R. ***G–K***, Stainings of embryonic NMJs (stage 17) for HRP (gray), GluRIIA (red), and GluRIIC (green). Blockade of synaptic transmission by expression of tetanus toxin light chain with the pan-neuronal driver *elav-gal4* (***I***) or by raising $shibire^{TS1}$ animals (***J***) at restrictive temperature led to embryonic lethality. However, proper clustering of glutamate receptors was observed (***G***). PSD assembly appeared also unaffected when $gluRIIA^{E783A}$ (see ***L***) was expressed in the $gluRIIA^{null}IIB^{null}$ background (***K***). A $gluRIIA^{hypo}$ NMJ (***H***) is shown for comparison. ***L***, Scheme of GluRIIA ^{E783A}, carrying a point mutation in the S2 glutamate binding domain resulting in embryonic lethality. Scale bars, 5 μm.

NMJ. To this end, a dominant-negative allele of Dynamin ($shibire^{TS1}$), which blocks both evoked as well as spontaneous synaptic transmission at restrictive temperature (Koenig et al., 1983), was used. To this end, after 12–14 h (AEL) at 25°C, embryos were transferred to 32°C 8–10 h before dissection. We found that PSDs (as judged by GluRIIA/GluRIIC costaining) formed apparently normally in $shibire^{TS1}$ mutants at restrictive temperature (Fig. 6*J*). The same result was obtained in embryos expressing tetanus toxin under control of the strong pan-neuronal driver *elav-gal4* (Fig. 6*I*). Together, apparently neither evoked nor spontaneous miniature responses were needed to allow normal postsynaptic assembly. Thus, it appeared unlikely that a general lack of postsynaptic conductance could underlie the postsynaptic defects at glutamate receptor-deprived NMJs. In fact, PAK accumulation at PSDs was even possible when a receptor-deprived situation ($gluRIIA^{hypo}$) was combined with a concomitant block of activity mediated by tetanus toxin (Fig. 5*H*).

We concluded that ionic conductance through postsynaptic glutamate receptors associated with neurotransmission did not appear to be a prerequisite for synapse assembly. Several studies have measured glutamate in the *Drosophila* hemolymph (Echalier, 1997). Thus, glutamate receptor conductance in response to such extracellular glutamate, not associated with vesicular release, could per se be implicated in synapse formation. However, genetic constellations meant to increase hemolymph glutamate levels were shown to decrease

the size of postsynaptic glutamate receptor fields (Featherstone et al., 2002), arguing against a PSD stabilizing role of such conductances in response to extracellular glutamate. Nonetheless, we tried to directly address the role of glutamate-mediated receptor conductance. First, a pore-modified *gluRIIA* genomic transgene (*gluRIIA*^{Q614R}) (Fig. 6*F*), changing the pore from MQQ to MRQ (Jonas and Burnashev, 1995; Kask et al., 1998; DiAntonio et al., 1999; Aronoff et al., 2004) was engineered. This rescued the *gluRIIA*^{null}*IIB*^{null} situation and allowed the formation of apparently normal receptor fields at larval NMJs (Fig. 6*E*). A "complete block" of NMJ transmission, however, should result in embryonic lethality, arguing that *gluRIIA*^{Q614R} does still allow some ionic conductance when incorporated into the glutamate receptor complex (DiAntonio et al., 1999).

In fact, embryonic rescue of the *gluRIIA*^{null}*IIB*^{null} situation was no longer possible with a GluRIIA mutated in the glutamate binding pocket (*gluRIIA*^{E783A}) (Fig. 6*L*) (Grunwald and Kaplan, 2003). However, at these embryonic *gluRIIA*^{E783A} NMJs, wild-type-like patches of the glutamate receptor subunits GluRIIA and GluRIIC formed at apparently normal density (Fig. 6*K*). Consistently, PAK kinase and presynaptic BRP also clustered normally at these synapses (data not shown), which should be most severely deprived of glutamate-triggered ionic conductance (also given that *gluRIIA*^{hypo} embryos survive despite the absence of detectable spontaneous responses). As a result, a lack of glutamate receptor-mediated ionic conductance is most unlikely to be responsible for the PSD defects observed at NMJ synapses lacking glutamate receptors. Instead, glutamate receptors might well be involved in postsynaptic assembly via protein–protein interactions.

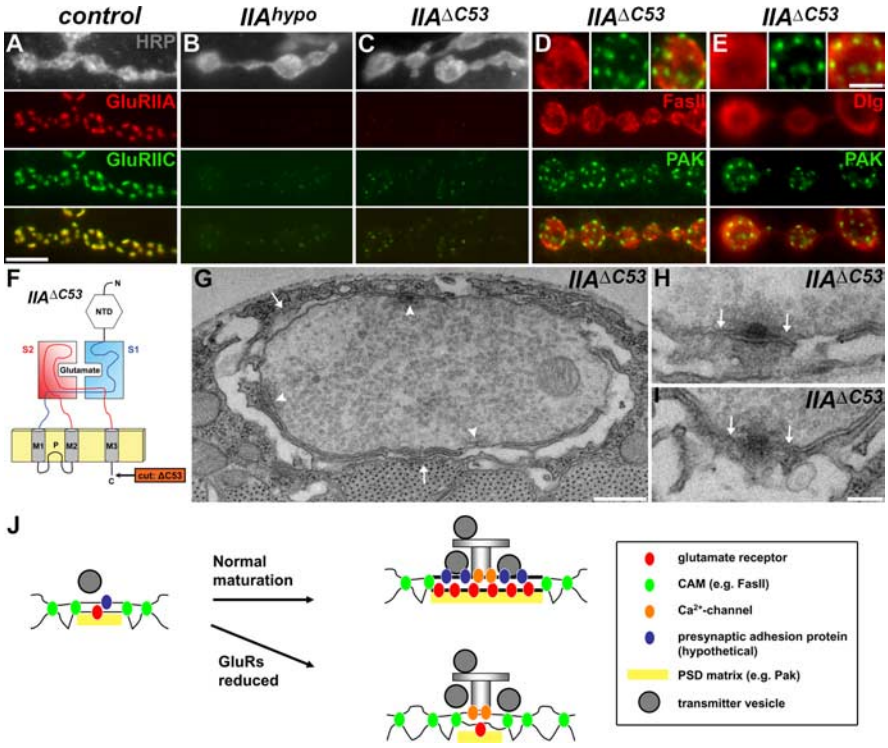

Figure 7. PSD assembly defects after C-terminal truncation of GluRIIA. ***A–C***, Epifluorescence images (recorded with equal illumination time) of third-instar NMJs stained for HRP (gray), GluRIIA (red), and GluRIIC (green). Expression of a truncated GluRIIA variant, missing the last 53 amino acids of the C terminus (*gluRIIA*$^{\Delta C53}$; see scheme in ***F***), in the *gluRIIA*^{null}*IIB*^{null} background (***C***) led to synaptic glutamate receptor levels similar as in *gluRIIA*^{hypo} (***B***) but severely reduced in comparison with controls (***A***) (wild-type genomic *gluRIIA* construct expressed in *gluRIIA*^{null}*IIB*^{null}). Boutons in *gluRIIA*$^{\Delta C53}$ were atypically round as observed in *gluRIIA*^{hypo} (***B***). ***D***, ***E***, *gluRIIA*$^{\Delta C53}$ NMJs stained for FasII (***D***; red) and Dlg (***E***; red). Similarly to *gluRIIA*^{hypo}, FasII and Dlg were no longer restricted from the synaptic membrane but rather evenly distributed over the bouton surface. PAK (green) accumulations as well were clearly decreased in size. ***F***, Schematic view of GluRIIA$^{\Delta C53}$. ***G***, Transmission electron microscopy of *gluRIIA*$^{\Delta C53}$ third-instar boutons uncovered a phenotype very similar to *gluRIIA*^{hypo}. While the formation of presynaptic T-bars persisted (arrowheads), the SSR was strongly reduced in overall thickness (arrows; wild type, 684 ± 55 nm, $n = 7$; *gluRIIA*$^{\Delta C53}$, 168 ± 30 nm, $n = 5$; $p = 0.0025$). ***H***, ***I***, Higher magnifications: often complete (***I***) or partial (***H***) lack of the electron dense character of presynaptic and postsynaptic membranes could be observed. The synaptic membrane apposition was either fully missing (***I***) or only partly established (***H***) at *gluRIIA*$^{\Delta C53}$ synapses (arrows). Scale bars: ***A***, 5 μm; ***E***, small panels, 2 μm; ***G***, 500 nm; ***I***, 200 nm. ***J***, Model: Maturation of PSDs requires glutamate receptors. Model shows the maturation of individual synapses with either normal or severely reduced/absent glutamate receptor levels. Initial definition of postsynaptic membranes (PAK accumulation) takes place even in the absence of glutamate receptors. However, additional expansion of postsynaptic membrane domains including recruitment of electron density at both presynaptic and postsynaptic membranes and evenly spaced adhesion between these membranes (apposition) fails when glutamate receptors are lacking. Thus, while presynaptic specializations mature, the PSD resides in an immature state and size with normally perisynaptic CAMs occupying principal PSD membranes.

C-terminal truncation of GluRIIA mimics the receptor deprivation defects

We sought to determine parts of the glutamate receptor proteins involved in synapse assembly and maturation. *gluRIIA* was deleted from its C terminus and a truncated genomic transgene (*gluRIIA*$^{\Delta C53}$) (Fig. 7*F*), missing the last 53 amino acids of the C terminus, but not the 3′-UTR, was expressed in the *gluRIIA*^{null}*IIB*^{null} background. Rescue capability of *gluRIIA*$^{\Delta C53}$ was lower than observed for *gluRIIA*^{hypo} (24 and 43% of expected mendelian rate of adult flies, respectively). Similar as found in *gluRIIA*^{hypo} (Fig. 7*B*), glutamate receptors at *gluRIIA*$^{\Delta C53}$ PSDs (Fig. 7*C*) were hardly detectable and drastically reduced (different from *gluRIIA*^{hypo} with only <5% of GluRIIA mRNA level left, the GluRIIA mRNA level of *gluRIIA*$^{\Delta C53}$ was not decreased) (data not shown). Alongside the reduction in synaptic glutamate receptors, NMJ morphology was clearly defective as well, harboring atypically round boutons (Fig. 7*C*). PSDs, visualized by labeling PAK, appeared decreased in size. As in *gluRIIA*^{hypo}, the perisynaptically expressed proteins FasII and Dlg were essentially evenly distributed over the bouton surface (Fig. 7*D*,*E*). Transmission electron micrographs showed a drastic drop in the overall thickness of the SSR (Fig. 7*G*, arrows) (wild type, 684 ± 55 nm, $n = 7$; *gluRIIA*$^{\Delta C53}$, 168 ± 30 nm, $n = 5$; $p = 0.0025$), and the number of membrane stacks appeared reduced. Importantly, membrane apposition in the synaptic region was only partly established or completely missing, and both presynaptic and postsynaptic membranes lacked electron-dense character (Fig. 7*H*,*I*). As for *gluRIIA*^{hypo}, presynaptic elements seemed unaffected (Fig. 7*G*).

In summary, the *gluRIIA*$^{\Delta C53}$ phenotype was very similar to the defects observed for *gluRIIA*^{hypo} (while even somewhat stronger). These data are consistent with the concept that a lack of interactions with other PSD components mediated by the intracellular C terminus interferes with PSD assembly. However, lack

of a C-terminal sequence could per se also affect initial transport and/or assembly of glutamate receptor complexes. In any case, this experiment independently shows that a lack of glutamate receptors interferes with the PSD assembly process.

Discussion

A detailed molecular and cell biological insight into the formation of glutamatergic synapses is important for understanding the development of excitatory neuronal circuits and also the process of long-term information storage in the CNS (Chklovskii et al., 2004). So far, studies on cultivated brain neurons analyzed mechanisms of glutamate receptor trafficking during synapse formation and have suggested a temporal sequence of presynaptic and postsynaptic assembly (Washbourne et al., 2002; Gundelfinger et al., 2003; Bresler et al., 2004). However, whether in turn the process of incorporating glutamate receptors is needed for the establishment of synaptic structures was hardly addressed.

A transmission-independent role of glutamate receptors in postsynaptic maturation

We addressed the relationship between neurotransmitter receptor incorporation and synapse assembly by genetically reducing or eliminating the expression of all neurotransmitter receptors at a certain synapse type. To our knowledge, consequences of eliminating all postsynaptic glutamate receptors expressed at a specific glutamatergic synapse had so far not been described. Here, we showed that a lack of glutamate receptors provoked a specific block in the molecular and ultrastructural maturation of PSDs.

Notably, loss of transmission concomitant with losing glutamate receptor complexes seemed not involved, based on the fact that neither blocking synaptic transmission (Fig. 6*C*,*D*,*I*,*J*) nor affecting glutamate binding by site-directed mutagenesis (Fig. 6*K*) did provoke similar defects. Thus, consistent with studies in other synaptic systems (Harris, 1980; Verhage et al., 2000; Baines et al., 2001; Misgeld et al., 2002; Varoqueaux et al., 2002; Heeroma et al., 2003), ionic transmission through the postsynaptic neurotransmitter receptors does not appear essential for principal synapse assembly. Instead, our data clearly imply that a critical level of glutamate receptor protein is needed to allow synapse maturation.

Ultrastructural and molecular maturation of NMJ synapses requires glutamate receptors

A model for the maturation of individual NMJ synapses in either the presence or absence of postsynaptic glutamate receptors is given in Figure 7*J*. At glutamate receptor-deprived synapses, synaptic vesicles appeared normally distributed, and their activity-mediated release appeared increased, likely as part of a compensation for reduced postsynaptic sensitivity. Moreover, functional active zones with presynaptic dense bodies still formed. Thus, active zones still assemble when the mature organization of synaptic membranes ("tight planar apposition") is not established. Consistently, previous work had shown that the formation of presynaptic dense bodies persisted even after genetic elimination of postsynaptic muscle cells (Prokop et al., 1996). In contrast, active zone formation is severely affected in *bruchpilot* mutants, whereas the presynaptic and postsynaptic membranes remain tightly apposed (Kittel et al., 2006; Wagh et al., 2006).

At developing NMJs, newly forming "nascent" PSDs are characterized by small GluRIIA accumulations strictly colocalized with PAK kinase (Rasse et al., 2005). Even in the complete absence of glutamate receptors (*gluRIIC* single or *gluRIIA&IIB* double mutant) (Fig. 5*E*,*F*), postsynaptic PAK patches, as typical for small nascent synapses, still formed, indicating that principal cues for the definition of postsynaptic membrane patches persisted in this situation. However, these PAK patches consistently failed to reach mature size (Fig. 3*J*,*K*). PAK, which mediates effects of Rho-GEF dPIX has been implicated in postsynaptic maturation, with PAK mutants showing a partial depletion of GluRIIA, and reduced SSR formation. However, neither *pak* nor *dpix* mutants have so far been reported to show defects in synaptic membrane apposition (Parnas et al., 2001; Albin and Davis, 2004). Thus, postsynaptic differentiation is not completely blocked in the absence of glutamate receptors. Instead, two postsynaptic "assembly modules" (PAK/dPIX signaling and glutamate receptor localization) appear only partly dependent on each other, with glutamate receptor localization being essential for PSD maturation but not for initial PSD assembly.

At the cholinergic mouse NMJ, genetic deletion of the adult acetylcholine receptor subunit ε (AChRε) led to severely reduced AChR density. Notably, a profound reorganization of AChR-associated components of the postsynaptic membrane and cytoskeleton was observed in this situation (Missias et al., 1997).

Glutamate receptor complexes and synaptic cell adhesion

Synaptic membranes are electron dense and apposed to each other, leaving a cleft of consistent width, likely essential for robust timing and efficacy of neurotransmission. In contrast, perisynaptic membranes are less electron dense and tend to undulate. At NMJs lacking glutamate receptors, FasII/Dlg complexes ectopically remained at synaptic sites and membranes now appeared undulated, indicating perisynaptic type of membrane adhesion. Thus, glutamate receptors seem essential to establish the type of membrane adhesion found at the synapse, whereas usually perisynaptic adhesion molecules as FasII mediate a qualitatively different type of membrane adhesion. Notably, undulation of perisynaptic membranes was impaired at NMJs lacking glutamate receptors leading to a less developed SSR (Figs. 4*D*,*K*; 7*G*). Moreover, boutons often appeared atypically round (Figs. 4*C*; 7*D*,*E*), further indicating that membrane–membrane adhesion is fundamentally affected at NMJ terminals lacking glutamate receptors.

Several classes of bona fide cell adhesion molecules (CAMs) have been implicated in mediating membrane adhesion at synapses, particularly transsynaptic neurexin–neuroligin pairs and cadherins (Murthy and De Camilli, 2003). The specific contributions of these synaptic CAMs during initial synapse assembly and maturation are under intense investigation. Our data are consistent with the idea that the C-terminal, intracellular domains of glutamate receptors might engage in interactions with other PSD components, which in turn cluster postsynaptic CAM-type membrane proteins. These would then mediate interactions to cluster presynaptic CAMs or bind components of the extracellular matrix to allow synaptic membrane apposition. Alternatively, direct interactions of glutamate receptors with other membrane protein complexes, as recently demonstrated for Stargazins/TARPs (transmembrane AMPA receptor regulatory proteins) (Osten and Stern-Bach, 2006), might be involved.

To our knowledge, no CAM single mutant has so far been reported to provoke a defect in synaptic membrane apposition as severe as the one observed here for glutamate receptor mutant situations. Thus, multivalent interactions of the heterotetrameric glutamate receptor complexes as well as the redundant involvement of several CAM species might occur.

Glutamate receptor levels in control of synapse formation

PAK labeling suggested that initial steps in defining postsynaptic membranes persisted even in the total absence of glutamate receptors, whereas these initial assemblies could not mature on the ultrastructural level when glutamate receptors were lacking. We recently achieved *in vivo* imaging of photolabeled GluRIIA at the developing NMJ, and found that newly forming PSDs in fact grow by a continuous incorporation of glutamate receptors, whereby the accumulation of presynaptic active zone material (BRP) appeared slightly delayed. Thereby, the entry of GluRIIA, likely derived from cell-wide plasma membrane pools via lateral diffusion, directly correlated with PSD growth. Once glutamatergic PSDs reached a certain size, they stabilized and GluRIIA was essentially immobilized. In comparison, other postsynaptic proteins showed high turnover equally over all synapses (Rasse et al., 2005). This slow turnover of glutamate receptors is consistent with the view that multiple interactions of glutamate receptor set the core of a transsynaptic interaction matrix. Several lines of genetic and experience-dependent manipulations point toward a rate-limiting role of GluRIIA levels in NMJ synapse formation (Broadie and Bate, 1993; Reiff et al., 2002; Sigrist et al., 2002; Yoshihara et al., 2005). In summary, the available data suggest that incorporation of glutamate receptors might be a key event to allow additional expansion of initial postsynaptic assemblies, finally leading to mature PSDs. Thereby, the overall level of glutamate receptors available in the muscle membrane might control the total number of synapses forming per NMJ (Rasse et al., 2005).

Understanding the plasticity processes taking place at glutamatergic synapses has been a focus of attention within cellular neuroscience. Hereby, rapid changes in synaptic receptor number were reported to mediate plastic changes of synaptic transmission, often on the timescale of tens of minutes in mammalian preparations (Malinow and Malenka, 2002; Sheng and Kim, 2002; Bredt and Nicoll, 2003; Collingridge et al., 2004). Notably, however, a recent study indicated that the cycling of synaptic glutamate receptors needed 16 h or more (Adesnik et al., 2005). Similar timing was observed for nicotinic acetylcholine and GABA receptors (Akaaboune et al., 2002; Thomas et al., 2005). Thus, parts of the synaptic glutamate receptor population might be needed to reside stably within the PSD to maintain synapse stability. In fact, only severe receptor deprivation interfered with proper postsynaptic assembly at the NMJ, suggesting that the glutamate receptor level should not fall below a certain critical threshold.

Notably, the extracellular domain of the mammalian AMPA receptor subunit GluR2 has been shown to increase the size and density of spines in hippocampal neurons, and to induce spine formation in GABAergic interneurons normally lacking spines (Passafaro et al., 2003). It will be interesting to see whether these structural roles of glutamate receptors have a common mechanistic denominator.

Different types of synapses differ strongly in the ultrastructural detail of their postsynaptic specializations. Thus, a typical neuron of our brain, acting as a postsynaptic partner for different types of presynaptic inputs, has to establish and maintain different postsynaptic architectures, suggesting the existence of "identity molecules" allowing the self-assembly of such architectures, and potentially a match with membrane cues of the presynaptic partner cell. Obvious candidates for such molecules are the postsynaptic neurotransmitter receptors themselves. This study is consistent with such a view.

References

Adesnik H, Nicoll RA, England PM (2005) Photoinactivation of native AMPA receptors reveals their real-time trafficking. Neuron 48:977–985.

Akaaboune M, Grady RM, Turney S, Sanes JR, Lichtman JW (2002) Neurotransmitter receptor dynamics studied in vivo by reversible photounbinding of fluorescent ligands. Neuron 34:865–876.

Albin SD, Davis GW (2004) Coordinating structural and functional synapse development: postsynaptic p21-activated kinase independently specifies glutamate receptor abundance and postsynaptic morphology. J Neurosci 24:6871–6879.

Aronoff R, Mellem JE, Maricq AV, Sprengel R, Seeburg PH (2004) Neuronal toxicity in *Caenorhabditis elegans* from an editing site mutant in glutamate receptor channels. J Neurosci 24:8135–8140.

Atwood HL (2006) Neuroscience. Gatekeeper at the synapse. Science 312:1008–1009.

Atwood HL, Govind CK, Wu CF (1993) Differential ultrastructure of synaptic terminals on ventral longitudinal abdominal muscles in *Drosophila* larvae. J Neurobiol 24:1008–1024.

Baines RA, Uhler JP, Thompson A, Sweeney ST, Bate M (2001) Altered electrical properties in *Drosophila* neurons developing without synaptic transmission. J Neurosci 21:1523–1531.

Barry MF, Ziff EB (2002) Receptor trafficking and the plasticity of excitatory synapses. Curr Opin Neurobiol 12:279–286.

Borgdorff AJ, Choquet D (2002) Regulation of AMPA receptor lateral movements. Nature 417:649–653.

Bredt DS, Nicoll RA (2003) AMPA receptor trafficking at excitatory synapses. Neuron 40:361–379.

Bresler T, Shapira M, Boeckers T, Dresbach T, Futter M, Garner CC, Rosenblum K, Gundelfinger ED, Ziv NE (2004) Postsynaptic density assembly is fundamentally different from presynaptic active zone assembly. J Neurosci 24:1507–1520.

Broadie K, Bate M (1993) Innervation directs receptor synthesis and localization in *Drosophila* embryo synaptogenesis. Nature 361:350–353.

Chen K, Merino C, Sigrist SJ, Featherstone DE (2005) The 4.1 protein coracle mediates subunit-selective anchoring of *Drosophila* glutamate receptors to the postsynaptic actin cytoskeleton. J Neurosci 25:6667–6675.

Chklovskii DB, Mel BW, Svoboda K (2004) Cortical rewiring and information storage. Nature 431:782–788.

Collingridge GL, Isaac JT, Wang YT (2004) Receptor trafficking and synaptic plasticity. Nat Rev Neurosci 5:952–962.

DiAntonio A, Petersen SA, Heckmann M, Goodman CS (1999) Glutamate receptor expression regulates quantal size and quantal content at the *Drosophila* neuromuscular junction. J Neurosci 19:3023–3032.

Dornan S, Jackson AP, Gay NJ (1997) Alpha-adaptin, a marker for endocytosis, is expressed in complex patterns during *Drosophila* development. Mol Biol Cell 8:1391–1403.

Echalier G (1997) *Drosophila*: cells in culture, Ed 1. New York: Academic.

Featherstone D, Broadie K (2002) Response: meaningless minis? Trends Neurosci 25:386–387.

Featherstone DE, Rushton E, Broadie K (2002) Developmental regulation of glutamate receptor field size by nonvesicular glutamate release. Nat Neurosci 5:141–146.

Garner CC, Zhai RG, Gundelfinger ED, Ziv NE (2002) Molecular mechanisms of CNS synaptogenesis. Trends Neurosci 25:243–251.

Gorczyca M, Popova E, Jia XX, Budnik V (1999) The gene mod(mdg4) affects synapse specificity and structure in *Drosophila*. J Neurobiol 39:447–460.

Grunwald ME, Kaplan JM (2003) Mutations in the ligand-binding and pore domains control exit of glutamate receptors from the endoplasmic reticulum in *C. elegans*. Neuropharmacology 45:768–776.

Gundelfinger ED, Kessels MM, Qualmann B (2003) Temporal and spatial coordination of exocytosis and endocytosis. Nat Rev Mol Cell Biol 4:127–139.

Harris WA (1980) The effects of eliminating impulse activity on the development of the retinotectal projection in salamanders. J Comp Neurol 194:303–317.

Heeroma JH, Plomp JJ, Roubos EW, Verhage M (2003) Development of the mouse neuromuscular junction in the absence of regulated secretion. Neuroscience 120:733–744.

Isaac JT (2003) Postsynaptic silent synapses: evidence and mechanisms. Neuropharmacology 45:450–460.

Jan LY, Jan YN (1976) Properties of the larval neuromuscular junction in *Drosophila melanogaster*. J Physiol (Lond) 262:189–214.

Jonas P, Burnashev N (1995) Molecular mechanisms controlling calcium entry through AMPA-type glutamate receptor channels. Neuron 15:987–990.

Kasai H, Matsuzaki M, Noguchi J, Yasumatsu N, Nakahara H (2003) Structure-stability-function relationships of dendritic spines. Trends Neurosci 26:360–368.

Kask K, Zamanillo D, Rozov A, Burnashev N, Sprengel R, Seeburg PH (1998) The AMPA receptor subunit GluR-B in its Q/R site-unedited form is not essential for brain development and function. Proc Natl Acad Sci USA 95:13777–13782.

Keshishian H, Broadie K, Chiba A, Bate M (1996) The *Drosophila* neuromuscular junction: a model system for studying synaptic development and function. Annu Rev Neurosci 19:545–575.

Kim E, Sheng M (2004) PDZ domain proteins of synapses. Nat Rev Neurosci 5:771–781.

Kittel RJ, Wichmann C, Rasse TM, Fouquet W, Schmidt M, Schmid A, Wagh DA, Pawlu C, Kellner RR, Willig KI, Hell SW, Buchner E, Heckmann M, Sigrist SJ (2006) Bruchpilot promotes active zone assembly, Ca^{2+} channel clustering, and vesicle release. Science 312:1051–1054.

Koenig JH, Saito K, Ikeda K (1983) Reversible control of synaptic transmission in a single gene mutant of *Drosophila melanogaster*. J Cell Biol 96:1517–1522.

Koh YH, Gramates LS, Budnik V (2000) *Drosophila* larval neuromuscular junction: molecular components and mechanisms underlying synaptic plasticity. Microsc Res Tech 49:14–25.

Kuromi H, Kidokoro Y (2002) Selective replenishment of two vesicle pools depends on the source of Ca^{2+} at the *Drosophila* synapse. Neuron 35:333–343.

Malinow R, Malenka RC (2002) AMPA receptor trafficking and synaptic plasticity. Annu Rev Neurosci 25:103–126.

Marrus SB, DiAntonio A (2004) Preferential localization of glutamate receptors opposite sites of high presynaptic release. Curr Biol 14:924–931.

Marrus SB, Portman SL, Allen MJ, Moffat KG, DiAntonio A (2004) Differential localization of glutamate receptor subunits at the *Drosophila* neuromuscular junction. J Neurosci 24:1406–1415.

Misgeld T, Burgess RW, Lewis RM, Cunningham JM, Lichtman JW, Sanes JR (2002) Roles of neurotransmitter in synapse formation: development of neuromuscular junctions lacking choline acetyltransferase. Neuron 36:635–648.

Missias AC, Mudd J, Cunningham JM, Steinbach JH, Merlie JP, Sanes JR (1997) Deficient development and maintenance of postsynaptic specializations in mutant mice lacking an "adult" acetylcholine receptor subunit. Development 124:5075–5086.

Murthy VN, De Camilli P (2003) Cell biology of the presynaptic terminal. Annu Rev Neurosci 26:701–728.

Osten P, Stern-Bach Y (2006) Learning from stargazin: the mouse, the phenotype and the unexpected. Curr Opin Neurobiol 16:275–280.

Parnas D, Haghighi AP, Fetter RD, Kim SW, Goodman CS (2001) Regulation of postsynaptic structure and protein localization by the Rho-type guanine nucleotide exchange factor dPix. Neuron 32:415–424.

Passafaro M, Nakagawa T, Sala C, Sheng M (2003) Induction of dendritic spines by an extracellular domain of AMPA receptor subunit GluR2. Nature 424:677–681.

Petersen SA, Fetter RD, Noordermeer JN, Goodman CS, DiAntonio A (1997) Genetic analysis of glutamate receptors in *Drosophila* reveals a retrograde signal regulating presynaptic transmitter release. Neuron 19:1237–1248.

Prokop A (1999) Integrating bits and pieces: synapse structure and formation in *Drosophila* embryos. Cell Tissue Res 297:169–186.

Prokop A, Landgraf M, Rushton E, Broadie K, Bate M (1996) Presynaptic development at the *Drosophila* neuromuscular junction: assembly and localization of presynaptic active zones. Neuron 17:617–626.

Qin G, Schwarz T, Kittel RJ, Schmid A, Rasse TM, Kappei D, Ponimaskin E, Heckmann M, Sigrist SJ (2005) Four different subunits are essential for expressing the synaptic glutamate receptor at neuromuscular junctions of *Drosophila*. J Neurosci 25:3209–3218.

Rasse TM, Fouquet W, Schmid A, Kittel RJ, Mertel S, Sigrist CB, Schmidt M, Guzman A, Merino C, Qin G, Quentin C, Madeo FF, Heckmann M, Sigrist SJ (2005) Glutamate receptor dynamics organizing synapse formation in vivo. Nat Neurosci 8:898–905.

Reiff DF, Thiel PR, Schuster CM (2002) Differential regulation of active zone density during long-term strengthening of *Drosophila* neuromuscular junctions. J Neurosci 22:9399–9409.

Rheuben MB, Yoshihara M, Kidokoro Y (1999) Ultrastructural correlates of neuromuscular junction development. Int Rev Neurobiol 43:69–92.

Richmond JE, Broadie KS (2002) The synaptic vesicle cycle: exocytosis and endocytosis in *Drosophila* and *C. elegans*. Curr Opin Neurobiol 12:499–507.

Saitoe M, Schwarz TL, Umbach JA, Gundersen CB, Kidokoro Y (2002) Response: meaningless minis? Trends Neurosci 25:385–386.

Salvaterra PM, Kitamoto T (2001) *Drosophila* cholinergic neurons and processes visualized with Gal4/UAS-GFP. Brain Res Gene Expr Patterns 1:73–82.

Schuster CM, Davis GW, Fetter RD, Goodman CS (1996) Genetic dissection of structural and functional components of synaptic plasticity. I. Fasciclin II controls synaptic stabilization and growth. Neuron 17:641–654.

Sheng M, Kim MJ (2002) Postsynaptic signaling and plasticity mechanisms. Science 298:776–780.

Sigrist SJ, Thiel PR, Reiff DF, Lachance PE, Lasko P, Schuster CM (2000) Postsynaptic translation affects the efficacy and morphology of neuromuscular junctions. Nature 405:1062–1065.

Sigrist SJ, Thiel PR, Reiff DF, Schuster CM (2002) The postsynaptic glutamate receptor subunit DGluR-IIA mediates long-term plasticity in *Drosophila*. J Neurosci 22:7362–7372.

Sigrist SJ, Reiff DF, Thiel PR, Steinert JR, Schuster CM (2003) Experience-dependent strengthening of *Drosophila* neuromuscular junctions. J Neurosci 23:6546–6556.

Stewart BA, Atwood HL, Renger JJ, Wang J, Wu CF (1994) Improved stability of *Drosophila* larval neuromuscular preparations in haemolymph-like physiological solutions. J Comp Physiol [A] 175:179–191.

Sweeney ST, Broadie K, Keane J, Niemann H, O'Kane CJ (1995) Targeted expression of tetanus toxin light chain in *Drosophila* specifically eliminates synaptic transmission and causes behavioral defects. Neuron 14:341–351.

Thomas P, Mortensen M, Hosie AM, Smart TG (2005) Dynamic mobility of functional GABAA receptors at inhibitory synapses. Nat Neurosci 8:889–897.

Thomas U, Kim E, Kuhlendahl S, Koh YH, Gundelfinger ED, Sheng M, Garner CC, Budnik V (1997) Synaptic clustering of the cell adhesion molecule fasciclin II by discs-large and its role in the regulation of presynaptic structure. Neuron 19:787–799.

Varoqueaux F, Sigler A, Rhee JS, Brose N, Enk C, Reim K, Rosenmund C (2002) Total arrest of spontaneous and evoked synaptic transmission but normal synaptogenesis in the absence of Munc13-mediated vesicle priming. Proc Natl Acad Sci USA 99:9037–9042.

Verhage M, Maia AS, Plomp JJ, Brussaard AB, Heeroma JH, Vermeer H, Toonen RF, Hammer RE, van den Berg TK, Missler M, Geuze HJ, Sudhof TC (2000) Synaptic assembly of the brain in the absence of neurotransmitter secretion. Science 287:864–869.

Verstreken P, Bellen HJ (2002) Meaningless minis? Mechanisms of neurotransmitter-receptor clustering. Trends Neurosci 25:383–385.

Wagh DA, Rasse TM, Asan E, Hofbauer A, Schwenkert I, Durrbeck H, Buchner S, Dabauvalle MC, Schmidt M, Qin G, Wichmann C, Kittel R, Sigrist SJ, Buchner E (2006) Bruchpilot, a protein with homology to ELKS/CAST, is required for structural integrity and function of synaptic active zones in *Drosophila*. Neuron 49:833–844.

Washbourne P, Bennett JE, McAllister AK (2002) Rapid recruitment of NMDA receptor transport packets to nascent synapses. Nat Neurosci 5:751–759.

Wucherpfennig T, Wilsch-Brauninger M, Gonzalez-Gaitan M (2003) Role of *Drosophila* Rab5 during endosomal trafficking at the synapse and evoked neurotransmitter release. J Cell Biol 161:609–624.

Yoshihara M, Adolfsen B, Galle KT, Littleton JT (2005) Retrograde signaling by Syt 4 induces presynaptic release and synapse-specific growth. Science 310:858–863.

Zhai RG, Bellen HJ (2004) The architecture of the active zone in the presynaptic nerve terminal. Physiology (Bethesda) 19:262–270.

Zito K, Fetter RD, Goodman CS, Isacoff EY (1997) Synaptic clustering of Fascilin II and Shaker: essential targeting sequences and role of Dlg. Neuron 19:1007–1016.